

# EVOLUTION SINCE $Z = 0.5$ OF THE MORPHOLOGY-DENSITY RELATION FOR CLUSTERS OF GALAXIES \*

Alan Dressler<sup>1</sup>, Augustus Oemler, Jr.<sup>1</sup>, Warrick J. Couch<sup>2</sup>, Ian Smail<sup>3†</sup>, Richard S. Ellis<sup>4</sup>, Amy Barger<sup>4</sup>, Harvey Butcher<sup>5</sup>, Bianca M. Poggianti<sup>4,5,6</sup> & Ray M. Sharples<sup>3</sup>

1) The Observatories of the Carnegie Institution, 813 Santa Barbara St., Pasadena, CA 91101-1292

2) School of Physics, University of New South Wales, Sydney 2052, Australia

3) Department of Physics, University of Durham, South Rd, Durham DH1 3LE, UK

4) Institute of Astronomy, Madingley Rd, Cambridge CB3 0HA, UK

5) Kapteyn Instituut, PO Box 800, 9700 AV Groningen, The Netherlands

6) Royal Greenwich Observatory, Madingley Road, Cambridge CB3 0EZ, UK

## ABSTRACT

Using traditional morphological classifications of galaxies in 10 intermediate-redshift ( $z \sim 0.5$ ) clusters observed with WFPC-2 on the Hubble Space Telescope, we derive relations between morphology and local galaxy density similar to that found by Dressler for low-redshift clusters. Taken collectively, the "morphology-density" relationship,  $T - \Sigma$ , for these more distant, presumably younger clusters is qualitatively similar to that found for the local sample, but a detailed comparison shows two substantial differences: (1) For the clusters in our sample, the  $T - \Sigma$  relation is strong in centrally concentrated "regular" clusters, those with a strong correlation of radius and surface density, but nearly absent for clusters that are less concentrated and irregular, in contrast to the situation for low redshift clusters where a strong relation has been found for both. (2) In every cluster the fraction of elliptical galaxies is as large or larger than in low-redshift clusters, but the S0 fraction is 2-3 times smaller, with a proportional increase of the spiral fraction.

Straightforward, though probably not unique, interpretations of these observations are (1) morphological segregation proceeds hierarchically, affecting richer, denser groups of galaxies earlier, and (2) the formation of elliptical galaxies predates the formation of rich clusters, and occurs instead in the loose-group phase or even earlier, but S0's are generated in large numbers only after cluster virialization.

*Subject headings:* cosmology: observations – clusters of galaxies: evolution

Received December 26, 1996; accepted July 15, 1997

---

\*Based on observations obtained with the NASA/ESA Hubble Space Telescope which is operated by STSCI for the Association of Universities for Research in Astronomy, Inc., under NASA contract NAS5-26555.

†Visiting Research Associate at the Carnegie Observatories.

## 1. Introduction

The observation that galaxy populations in clusters differ from those in the field goes back at least as far as Hubble & Humason (1931). Both Spitzer & Baade (1951) and Gunn & Gott (1972) suggested that dynamical processes within clusters might be responsible for transforming populations of spiral galaxies into S0's. In a study of 10 rich clusters, Oemler (1974) found that the cluster population was a function of both cluster structure and location within the cluster. Regular, centrally concentrated clusters, whose appearance suggests that they are dynamically relaxed, have large populations of E's and S0's, small numbers of spirals, and strong radial population gradients, with the ratio of early-to-late-type galaxies increasing towards the center. Irregular, unrelaxed-looking clusters have populations that are much more spiral-rich and show no signs of radial gradients. Oemler suggested, following Gunn and Gott, that the high S0/spiral ratio in relaxed clusters was due to dynamical processes within the clusters, but that the enhanced abundance of E's in the most centrally concentrated clusters, which are often dominated by cD galaxies, was due to an enhanced formation rate of ellipticals at early times in the densest environments that would later become the cores of rich clusters.

Dressler (1980a, hereafter D80) used data for  $\sim 6000$  galaxies (Dressler 1980b, hereafter DCAT80) to investigate correlations between morphological type, cluster properties, and spatial distribution in 55 low-redshift rich clusters. Dressler correlated the spiral, S0, and elliptical fractions with the *local* surface density of galaxies, defined in a rectangular area containing the 10 nearest neighbors. He found a smooth, monotonic relation, now commonly known as the *morphology–density relation*, actually a correlation with surface density, which we will refer to here as the  $T - \Sigma$  relation. Dressler concluded that, to first order at least, the  $T - \Sigma$  relationship was universal, that is, representative of every cluster in the sample, regardless of its global properties. (Indeed, other workers (e.g. Geller & Beers 1982) have claimed that it extends beyond cluster environments into the general field population.) Of particular importance was Dressler's finding that, while irregular clusters showed no radial segregation of cluster populations, as Oemler had shown, they did display a  $T - \Sigma$  relation as strong as that of regular, concentrated clusters. Of course, the finite number of galaxies in each cluster prevents the testing of this hypothesis on a case-by-case basis, so that this conclusion was reached by combining together the data for regular, centrally-concentrated clusters and comparing them to those of irregular, clusters of low central concentration.

Both Oemler's and Dressler's portrayals of cluster populations are consistent with environment playing a critical role in determining present galaxy populations. Indeed, for relaxed, centrally-concentrated clusters the two descriptions are equivalent, because there is a one-to-one correspondence between radial position and local density in such clusters. However, the difference for irregular clusters is significant. Were irregular clusters to show little segregation by type, it would be reasonable to conclude that evolutionary processes which transform galaxies only work in the environment of a massive, relaxed system. On the other hand, finding local correlations between environment and populations even in small, cold subsystems suggests that much more local processes are at work.

The purpose of this paper is to investigate these issues in clusters at higher redshift,  $z \sim 0.5$ , in order to trace the evolution of galaxy populations in clusters, specifically the processes that might alter galaxy types and/or be responsible for their spatial distribution within clusters. This paper is one of a series analyzing the data obtained by the “MORPHS” group using the WFPC-2 on the Hubble Space Telescope. We have imaged 11 fields in 10 clusters of galaxies in the redshift range  $0.36 < z < 0.57$  and cataloged the positions, photometric data, and morphological classifications for 1857 objects brighter than  $R = 23.5$  or  $I = 23.0$ , as described in Smail et al. (1996a, hereafter, S97a). Although the addition of further parameters derived from spectroscopy of these galaxies, such as cluster or field membership, internal dynamics, stellar population, and cluster dynamics, are likely to be revealing as to the evolutionary state of these populations, photometric/morphological information alone allows a simple and important comparison with the properties of present day clusters. This comparison offers clues as to how clusters of galaxies came to hold their atypical complements of galaxy types.

The paper is organized as follows: In section 2 we briefly review the data used for this study. In Section 3 we revisit the relation between morphology and surface density introduced in D80. We include a short discussion of subsequent challenges to the original work, which is further explored in the Appendix. Section 4 gives our results for the higher-redshift sample, and in Section 5 we suggest some possible conclusions about galaxy evolution in clusters that might be drawn from our results.

## 2. A Brief Review of the Data

As described in S97a, our data consist of images of 11 fields of 10 rich clusters, obtained with the WFPC-2 on the Hubble Space Telescope. The exposures are typically 4 to 6 orbits each of  $\sim 2000$  s duration. In a few cases fields were observed in more than one band, but for the purposes of this paper only F814W or F702W exposures are involved, since these alone were used for morphological classification. By inspecting the images in what is essentially the rest-frame B-band, we have tied our system to the Revised Hubble and de Vaucouleurs schemes, which are traditionally based on images in the B-band — this mitigates legitimate concerns about type-dependent  $k$  corrections. The morphological classifications used here follow the traditional method of visual inspection of images. As discussed in S97a, at least two, and often three or four of us assigned a morphological type for an image, with a high degree of repeatability and consistency.

The clusters in our sample were not selected through any systematic criteria, but represent many of the best examples of well-studied clusters at intermediate redshift. As such, they are all rich (populous) clusters, though with a range in richness of a factor of three. They also represent a range in dynamical state, as evidenced by the regularity of the spatial distributions of their galaxies: the clusters range in appearance from highly concentrated and regular to very chaotic and dispersed. A further indication of their diversity of properties is the order-of-magnitude spread in their masses and X-ray fluxes (Smail et al. 1997b). This is not to say that our small

sample spans the distribution of richness and types that are characteristic of the Abell catalog, for example, but not all of the clusters are analogs or richer versions of such unusual low-redshift clusters as Abell 1656 (the Coma cluster) or Abell 2029.

The images cover the central 0.4–0.8  $h^{-1}$  Mpc for a  $q_0 = 0.5$  and  $h = H_0/100$  km sec $^{-1}$  Mpc $^{-1}$  cosmology, for which 1 arcsec is equivalent to 3.09  $h^{-1}$  kpc for our lowest redshift cluster and 3.76  $h^{-1}$  kpc in the most distant. For a resolution approaching 0.1 arcsecond, then, these images show detail at the level of  $\sim 500$  pc, equivalent to observing galaxies in the Coma cluster with 1" seeing. While cruder than the resolution usually available for morphological classification of nearby galaxies, this is sufficient for the identification of basic morphological information — the presence of disks and bulges, and large-scale spiral arms, dust lanes, and bars. In particular, this resolution is comparable to that obtained in the D80 study of morphology in low-redshift clusters, for which  $z = 0.04$  and 1" seeing were the norm.

Object identification and measurement of photometric parameters were accomplished using a modified version of the SExtractor image analysis package (Bertin & Arnoult 1996). Because of the low sky background and long integration times, the exposures go very deep, to a  $5\sigma$  limiting depth of  $I_{814} \simeq 26.0$  or  $R_{702} \simeq 27.0$ . However, after considerable testing, including intercomparisons of our several human classifiers, we concluded that reliable classification could not be done fainter than  $R_{702} = 23.5$  or  $I_{814} = 23.0$  with these images. In fact, as discussed below, for the purposes of the analysis described here, we reached this limit only for the highest redshift clusters. In S97a there is a detailed discussion of how the morphological classifications were assigned and what is their inferred accuracy.

For the purposes of this work, only the objects which were given Revised Hubble types were used; galaxies that appeared extremely chaotic or insufficiently detailed to fit into one of the categories — a few percent in all — were not included. This results in a small inconsistency with what has been done in studies of lower redshift clusters, for which galaxies were all assigned to one type or another, but we believe it is the safest thing to do for the classifications of distant samples. It is certainly not the case that all of this few percent of cases belong to one class, for example, the irregulars. Probably half are cases of bulge-dominated, earlier types whose division into elliptical, S0, and spiral cannot be made because of too few pixels in an image. Of the extremely chaotic systems, we believe that most of these should not be put into the irregular class, since they are much rarer at the present epoch and, as such, have no counterparts in the Revised Hubble scheme. (The “irregular” class in the Revised Hubble system refers to a specific morphological type, and was not intended as a repository for galaxies that did not fit into the other classifications.)

### 3. The Morphology-Density Relation, Revisited

Following Oemler (1974), Melnick and Sargent (1977) found a strong gradient in morphological type with radial distance, what we will here refer to as a T-R relation, for a sample of clusters with strong thermal X-ray emission, in the sense of spiral fraction increasing outwards and elliptical

and S0 fractions increasing inwards. As is typical of luminous X-ray clusters, these were centrally concentrated clusters with “regular” (non-clumpy) galaxy distributions. The DCAT80 sample of 55 clusters with  $z \sim 0.04$  contained examples of this type, all of which showed strong radial population gradients. In addition, however, this sample included many irregular clusters with poorly defined centers and low concentration. As Oemler had found, radial gradients for these were weak or even absent; multiple centers often complicated the attempt to look for such trends. However, because such clusters often were found to contain several higher density clumps with increased fractions of E and S0 galaxies, Dressler was led to look for a correlation of galaxy type with the local density, as discussed in Appendix 1.

The basic interpretation of the  $T - \Sigma$  relation was that the environmental density, possibly reaching back to quite early epochs, might have exercised substantial influence on the evolution of morphological types. At the time this might have been considered surprising, since it was commonly argued that galaxy mixing in the virializing collapse of a cluster would remove any correlation of a galaxy with its previous environment. However, subsequent N-body simulations confirmed that simple “top hat” analytical models of cluster virialization were misleading because the more realistic N-body models of structure growth showed that mixing was far less thorough. In fact, the simulations showed that galaxies found at the present epoch in high density regions were more than likely to have been in higher density regions throughout their lifetimes, even if there had been considerable mixing of the individual galaxies with those from somewhat lower density environments (see, e.g., Evrard, Silk, & Szalay 1990).

The data from DCAT80 have been reanalyzed for the purposes of this paper. Following Whitmore, Gilmore, and Jones (1993), we have made a field correction that is dependent on morphological type, in addition to correcting the local surface density for field contamination. The percentages 18/23/59 adopted by these authors for field E/S0/S+I contamination have been adopted here as well. This produces a small but noticeable change — in particular it lowers the spiral fraction at the lowest projected densities, since many of these are in fact projected field galaxies not associated with the cluster. We have also made finer divisions in binning the data, now 0.2 dex in surface density, to make full use of the large, statistical sample. This revised version of the D80 morphology-density relation for the entire 55 cluster sample is shown in histogram form in Fig. 1. Also shown in Fig. 1, and in subsequent  $T - \Sigma$  plots, is the number histogram of the membership in each bin. This is useful for estimating when the fractions in individual bins are very uncertain, i.e., when fewer than 10 galaxies comprise a bin. However, here we mean to compare only overall trends and not individual bins, so we have chosen to omit error bars for each bin, as they greatly confuse the diagrams. (We have, however, tabulated these values and their errors in tables as Appendix 2.) The noise due to counting statistics can be judged by the scatter from one bin to the next of what would otherwise likely be monotonic relationships.

Subsequently, the  $T - \Sigma$  relation was studied for poorer groups and the field (Bhavsar 1981, de Souza et al. 1983, Postman & Geller 1984, Giovanelli, Haynes, & Chincarini 1986) with the general result that the trends found for rich clusters were found to continue to lower density environments, with lower precision due to the uncertainties of projection effects for low-density environments. However, Salvador-Sole et al. (1989) pointed out that if the  $T - \Sigma$  relation were

universal for surface densities, as D80 had suggested, then the relationship between morphology and three-dimensional space density could not be universal, implying that a further dependence on some more global property, one that compared whole clusters with one another, might also play a role. In fact, Dressler had suggested that his sample showed some evidence for a global dependence on cluster concentration by noting a shift of the population levels for the clusters with the strongest X-ray emission. Salvador-Sole et al. pointed out that the sense of this effect, if real, was to imply an even greater dependence on concentration in the three-dimensional correlation. Though this analysis might be questioned because of its reliance on a smooth power-law model for the distribution of galaxies in the cluster, both results seemed to point to some additional determinant of cluster population beyond the local density, perhaps connected with a global property of the cluster.

The case for a dependence on cluster populations with a global cluster property was prosecuted even more vigorously by Whitmore & Gilmore (1991) and Whitmore, Gilmore, & Jones, (1993), who argued that the *sole* determinant of galaxy type within rich clusters is the radial distance from the cluster center (a T-R relation) to the exclusion of local density or even any other global property, such as X-ray luminosity, velocity dispersion, or central density. A thorough examination of this approach by Whitmore and collaborators is beyond the scope of the present paper, but we include in this paper in Appendix 1 a discussion of additional evidence that bears on this question of whether local density or radial distance from the cluster center is better correlated with morphological type.

Although we will show both  $T - \Sigma$  and T-R relations for our distant clusters, our emphasis will be on the former. In particular, we divide our sample into centrally-concentrated, regular clusters and low-concentration, irregular clusters. A comparison of these two kinds of clusters in the DCAT80 sample continues to provide the best evidence that the  $T - \Sigma$  relation is a manifestation of a genuine physical process operating in clusters that relates environmental density to galaxy morphological type, either causally or through a common connection. We show such data in Fig. 2a for 10 of the most centrally concentrated and Fig. 2b for the lowest-concentration clusters. The global properties of these samples are very different: velocity dispersions and x-ray fluxes are much higher for the centrally concentrated clusters, and of course, cluster centers are well defined in these but not in the low concentration clusters. Nevertheless, the  $T - \Sigma$  relations for both kind of clusters look very similar, with a strong dependence of spiral and elliptical fraction with local density for both. As we show in the Appendix, the increase in elliptical fraction with  $\Sigma$  is, within the errors, the same in both, although there might be a significant excess of S0's, and corresponding smaller spiral fraction, in the centrally-concentrated clusters compared to the low-concentration clusters. This may be indicative of an additional factor other than local density influencing cluster populations, but these differences are marginally significant at best.

Because the  $T - \Sigma$  relation is evident for low-redshift clusters of all types, we use it as the basis for analyzing the  $T - \Sigma$  relation for the intermediate-redshift clusters of our sample. While global influences may also play a role for low-redshift clusters, the evidence continues to support the conclusion that local density and morphological type are strongly connected.

#### 4. The $T - \Sigma$ Relation at $z \sim 0.5$

We now turn to the subject of how the  $T - \Sigma$  or T-R relations are manifest in our sample of 10 intermediate-redshift clusters at  $z \sim 0.5$ . A list of these clusters, their positions, and redshifts are given in Table 1. We will assume that our morphological classifications are made comparably to the DCAT80 study of 55 nearby clusters, that is, that the ability to discern salient features for classification are not appreciably diminished for these more distant clusters. With the possible exception of a difficulty in distinguishing face-on S0 from elliptical galaxies, a problem even for nearby galaxies, we believe that this assumption is justified, as discussed in S97a. (We also discuss this issue further below.) As in DCAT80, our classifications of morphological types in the intermediate-redshift clusters include cases designated E/S0 and S0/E. As explained in S97a, the order reflects the preference in the classification. Therefore, as done in that study, we have added these types into E and S0, respectively.

As in D80, the analysis of the  $T - \Sigma$  relation for the DCAT80 sample was done for galaxies down to a fixed apparent magnitude limit  $V = 16.5$ , which corresponds to  $M_V = -20.4$  for  $H_o = 50$  and  $z = 0.040$ . We have chosen  $M_V = -20.0$  as the magnitude limit of the  $T - \Sigma$  analysis of our clusters at intermediate redshift. Using standard Kron-Cousins/Johnson filter transmissions, the energy distribution of an Sbc galaxy, and conversions from F702W to R and F814W to I given by Holtzman et al. (1995), we have derived the magnitude limits given in Table 1. Also in Table 1 we give the number of galaxies in each cluster brighter than the magnitude limit, and the fractional representation of the different morphological types for each field, corrected for field contamination. We obtained values of Galactic extinction for each cluster from NED; the maximum of these corresponds to 0.23 mag in the F702W band observation of CL0303+17. These small corrections to the limiting magnitude have not been made, as also was the choice in D80. They make no significant change to the fractional distributions of the populations.

We also need to take note of the fact that our intermediate-redshift sample is studied over a smaller area (by a linear factor of approximately 2.5) than that of the low-redshift sample of DCAT80. We have therefore reanalyzed the data for the 55 clusters for a restricted area — a box that is 1094 arcsec on a side, or 1.2 Mpc ( $H_o = 50$ , adopted in D80), for  $z = 0.040$ , and scales with redshift. For most of the low redshift clusters we have centered the box on the plate center, but have used the “local density peak” centers (see Appendix 1) for the centrally concentrated and low concentrated subsamples. The  $T - \Sigma$  relation for the whole sample, and for the centrally concentrated and low concentration samples, are shown in Fig. 3a-c, respectively. There is no obvious difference between these and Figs. 1 & 2, except that the lowest density range is unpopulated, as expected, and that the statistics for the two subsamples are substantially degraded, especially for the low concentration sample.

We have applied a field correction, taken from the Medium Deep Survey (Griffiths et al. 1994), of 11.2 gal/sq arcmin at  $I = 23.0$ . As we did for the 55 cluster sample, we have made differential corrections by type to the counts in the distant clusters. We adopt the percentages of the different types found in the Medium Deep Survey — 10%, 10%, and 80% for elliptical, S0, and spiral galaxies, respectively (S97a). These values are, coincidentally, the same as used by

D80, which have been replaced here in our reanalysis of the DCAT80 sample with the Whitmore, Gilmore and Jones’s values of 18%, 23%, and 59%). There is no reason or expectation for using the same values for both low- and intermediate-redshift clusters, since the resolution of the images, and the composition of the field contamination are not necessarily the same.

We now compare Fig. 3a (or, equivalently, Fig. 1) to the  $T - \Sigma$  relationship for the entire  $z \sim 0.5$  sample, Fig. 4, noting first that, while there is considerable overlap in density between the two samples, the density range encompassed by the more distant sample is shifted by half a dex to higher density. This undoubtedly reflects the fact that these clusters are systematically richer than the *typical* clusters of DCAT80, although there is considerable overlap with the projected density range covered by that sample. Specifically, 13% of galaxies in the DCAT80 sample lie at  $\Sigma < 1.2$  lower limit of the intermediate redshift sample, and 12% of this sample are found at  $\Sigma > 2.5$ , a higher projected density than found in any of the DCAT80 clusters. Because 75% of the galaxies in the two samples share the same range in projected density range (somewhat greater if  $q_0 \ll 0.5$ ), we do not consider these two samples as composed of qualitatively different kinds of clusters. (For example, CL1601, CL0054, and Cl0303, share the density range of the DCAT80 sample.) It would be desirable, of course, to include more clusters typical of the present epoch in future samples.

Before addressing the question of gradients in Fig. 4, we take note of the obvious differences between this and the nearby cluster sample. As is now well known, spirals are greatly overabundant in high density environments compared to present-epoch clusters, but, perhaps surprisingly, the difference seems to be made up entirely by a paucity of S0 galaxies rather than an underabundance of *both* S0 and E galaxies. In fact, E galaxies appear to be in even greater abundance than in the nearby sample! In the overlapping density regimes of Fig. 3a and Fig. 4, spirals are a factor of 2 overabundant, S0’s are a factor of 2–3 underabundant, and ellipticals are a factor of 1.5 overabundant. The E or S0 population is, of course, little affected by the uncertainty in the correction for field galaxies, since galaxies of this type make up a small ( $\sim 20\%$ ) fraction of the intermediate-redshift field population.

In order to further investigate the possibility of misclassifications of E and S0 galaxies we have, as explained in S97a, compared the distribution in flattenings of S0 galaxies in our sample with that for the Coma cluster, in an attempt to see if we have misclassified S0 galaxies as ellipticals, particularly for the face-on cases. The good agreement of these distributions indicates that this is not the case. Our best estimate is that we have misclassified as ellipticals approximately 12% of the total S0 population that is nearly face on. As discussed in S97a, this has been determined through comparison with the Revised Shapely Ames galaxies (as tabulated in Sandage, Freeman, and Stokes 1970), but we believe that in comparison with classifications of nearby clusters, such as DCAT80, the degree of misclassification is so similar as to make any systematic differences negligible. We demonstrate this in Fig. 5, where we compare the distribution of ellipticities for both E and S0 in the  $z \sim 0.5$  cluster sample with the E and S0 galaxies in the Coma cluster (Andreon et al. 1996) and 11 clusters from DCAT80 with  $0.035 < z < 0.044$ . In both cases the distributions are in very good agreement, suggesting that any *differential* comparison of the E and S0 fractions in these clusters is justified. We thus conclude that the substantial difference seen in



the S0/E fraction in distant clusters compared to nearby clusters is genuine for this sample; of course, verification in a larger sample, to be certain that our sample is truly representative, would be highly desirable. The implications of this difference in E and S0 populations is discussed in Section 5.

We now ask whether any trend of morphology with density is apparent for the distant sample. From Fig. 4 it appears that a modest  $T - \Sigma$  relation is present, but it is only for the bins of highest density — over the last factor of 5 in surface density. Over this range the spiral fraction plummets and the elliptical fraction rises sharply, but for the lower density zones, over which there is a very noticeable gradient in the nearby clusters, the relationships are basically flat. Slicing the sample by redshift or richness does not change this result. However, when the sample is divided by the cluster concentration, which correlates well with degree of regularity, a very different picture emerges. We have used Butcher & Oemler’s (1978) definition of concentration as  $\log(R_{60}/R_{20})$ , where the latter refer to the radii containing 60% and 20% of the cluster populations, respectively. These values are given in Table 1 under the heading “Conc.” Fig. 6 shows the  $T - \Sigma$  relation for the four clusters of the  $z \sim 0.5$  sample with the highest central concentration — 3C295, Cl0024+16, Cl0016+16, and Cl0054–27. The  $T - \Sigma$  relation for this subset is steep and well defined over the entire density range, as strong as the  $T - \Sigma$  relation for the low redshift sample. As expected, the T-R relation (Fig. 7), being more-or-less degenerate with  $T - \Sigma$  for these cases, is also very strong for these clusters. Though the gradients in Fig. 6 are as strong as that found for low-redshift clusters, there are substantial differences, of course. Most obvious is the prevalence of spiral galaxies even in very high density regions. And although the S0 galaxies show the same flat distribution in projected density, they are, as we have pointed out, far less abundant. Finally, in comparison with Fig. 3, Fig. 6 appears to show a 5–10% excess of elliptical galaxies at the same surface density, extending to much higher fractions, at higher density, than has been found for lower redshift clusters. This may again highlight the unusual richness of some of the high redshift clusters in this sample.

The remaining clusters of lower concentration — Cl0303+17, Cl0412–65, Cl0939+47, Cl1447+23, Cl1601+42 — have irregular, clumpy distributions of galaxies, just like their low redshift counterparts. We show in Fig. 8 that, in contrast with the relatively strong gradients seen for the centrally concentrated clusters, there are no correlations at all for these 5 lowest-concentration, irregular clusters, except perhaps for a small *anticorrelation* of low statistical significance.<sup>‡</sup> (The T-R relation is, of course, nonexistent as well.) Apparently, then, the morphology-density relation is well established at higher redshift for the clusters that appear well evolved dynamically, but there is no apparent segregation in clusters that have more chaotic distributions. Of course, even the equivalent diagram for the centers of low- $z$  clusters of low concentration (Fig. 3c) suffers from small number statistics, so it is possible that this is an unrepresentative sample. We note however, that although the population gradients are not evident in the high- $z$ , low-concentration clusters, the elliptical fraction is high and the S0 fraction is

---

<sup>‡</sup>We have omitted the outer regions of two clusters, A370 and Cl0939+47, cataloged in S96. The central region of Cl0939+47, a low concentration cluster, is included in our analysis here, but equivalent morphological classifications using WFPC-2 for the center field of A370, a centrally concentrated cluster, are not yet available.

very low, as it is for the high- $z$ , high-concentration clusters and the low- $z$  sample. It is only the arrangement of these galaxies within the clusters, and not their relative proportions, that seems to differ from the centrally concentrated clusters.

These, then, are our principal results from the small sample of intermediate redshift clusters we have studied. (1) Over the range of density studied, which extends to somewhat higher densities, on average, than for the typical nearby cluster, elliptical galaxies are present in numbers comparable to what is seen today, while spirals are much more abundant and S0 galaxies much less abundant. (2) There is a modest  $T - \Sigma$  relation, but only for the highest densities, when all the clusters are taken together. (3) When the sample is divided into high-concentration, regular clusters and low-concentration, irregular clusters, the former show strong gradients in morphology over the represented range in surface density, but the latter show no gradients at all.

## 5. Discussion

Perhaps the most striking result of this study is that, whether the clusters appear dynamically “mature” or not, the incidence of elliptical galaxies is already very high. Put another way, the elliptical fraction is high whether or not ellipticals are collected into dense, central regions. This suggests that elliptical galaxies predate, and are basically independent of, the virialization of a rich cluster.

Supporting evidence for the idea that elliptical galaxies in rich clusters are old can be found in the Ellis et al. (1996) study of the  $(U - V)_o$  colors of these same ellipticals. Ellis et al. concluded, based on a scatter in rest frame  $U - V$  color of 0.07 mag — scarcely larger than the value of 0.035 mag found for ellipticals in the nearby Coma cluster (Bower, Lucey, & Ellis 1992) — that the stars in cluster elliptical galaxies formed early,  $z \gtrsim 3$  (or that, if they formed later, they formed within a very small time). This seems to argue against a “late-merger” origin for ellipticals, or at the least against dissipative mergers of star forming systems. In fact, as we will explore elsewhere, those systems in our sample for which a merger is likely to have “recently” occurred are still, for the most part, disk systems; therefore, most are unlikely to be the ancestors of elliptical galaxies because there is no expectation that the disk will be destroyed without another significant encounter. We have further evidence of this in their distribution within the clusters: when we plot the fractional population of highly asymmetric or disturbed morphologies (all morphological types with  $D > 1$ , as defined in S97a) with local surface density (Fig. 9), we see that these follow the S0 or spiral trend rather than the trend for ellipticals.<sup>§</sup> That is, the fraction of asymmetric galaxies is decreasing, or perhaps flat, but certainly not rising, with increasing density. This is a result similar to that found by Oemler, Dressler, and Butcher (1997) for the distribution of “disturbed” galaxies in four distant clusters.

Taken together, these three observations — the prevalence of E galaxies, their small  $U - V$

---

<sup>§</sup>The density range extends to lower values than previously because no attempt has been made at a field correction.

scatter, and the fact that most of the disturbed galaxies are disk systems and likely to remain so — suggest that, at least for the environments of rich clusters, elliptical galaxies are not the result of mergers of star-forming, gas-rich systems after a redshift  $z \sim 3$ . This does not preclude the possibility of dissipationless mergers at  $z \sim 1$ , say, when these clusters might have been in the process of accreting small groups with lower velocity dispersion, but both the distribution and numbers of ellipticals we have found here, and their photometric and spectral properties, suggest that ellipticals in these regions are not produced by late mergers, or in any process that depended on the dynamical evolution of a rich cluster. Instead, gaseous mergers or coherent collapse at high redshift, or growth of spheroids through dissipationless mergers continuing until later epochs, seems to be the history indicated for ellipticals. It is remarkable, we think, that the environments of proto-clusters of this richness were able to produce such a large population of ellipticals before the identities of the clusters themselves were well established.

The situation for the S0 galaxies seems to be just the opposite. Though the ones we find are, like the ellipticals, red and with little scatter in color, their numbers are so deficient as to suggest that many need to be added since  $z \sim 0.5$ , in order to reach the populations of present-epoch clusters. The source of these S0's seems clear: the overabundance of spirals provides a reservoir of galaxies which may be stripped by ram pressure, tidally harassed (Moore et al. 1995) merged, or subjected to strong 2-body gravitational interactions, with the result of producing today's dormant disk galaxies in clusters. As we will describe in more detail in a later paper, our  $z \sim 0.5$  cluster sample includes a significant number of disturbed, distorted morphologies, often with spectroscopic evidence of strong episodes of recent — in a few cases current — star formation. These may be the result of mergers, strong interactions, accretions, harassment, or stripping — we are still unable to tell which of these processes are responsible. But, as we have said, we do know from our morphological classifications that most of these are disk systems — they do not seem destined to settle into luminous elliptical galaxies when their jostling and bursts of star formation have ceased. Though the exact mechanism(s) may be yet unspecified, it seems that at least half of the S0 galaxies in today's clusters have been made by such processes since  $z \sim 0.5$ . Some support for this model may also be found from the trend of the S0/E ratio with redshift, which we show in Fig. 10. Omitting the two outer fields, which are properly excluded for this analysis, we see what appears to be a significant trend of increasing S0 abundance with decreasing redshift. Even more provocative is the observation that this trend, in linear extrapolation, comes close to predicting the S0/E ratio of  $\sim 2$  found in the D80 study of clusters at low redshift. Although these data are of too low statistical weight to be conclusive, they suggest that we could be seeing the process of S0 production over the interval in cosmic time probed by these observations.

On the other hand, according to Ellis et al. (1996), the spread in rest frame  $U - V$  colors for S0 galaxies in these clusters is as small as it is for ellipticals, from which it was concluded that the stellar populations in ellipticals are very old. While we may with the present data simply postulate that these represent a population of old S0's that formed with the ellipticals, our suggestion that most of the S0's in these clusters have yet to form means that the color spread at some later time, at  $z \sim 0.2$ , for example, should be significantly larger, reflecting the more recent evolution of these systems from previously star forming galaxies. To make comparable morphological classifications in clusters at this redshift will require either a mosaic coverage with HST or larger-field CCD

imaging with ground based images under conditions of superb seeing.

At first glance it may not be surprising, then, to see a  $T - \Sigma$  relation for the dynamically well-evolved clusters of our sample. One can imagine a large initial population of elliptical galaxies, formed at some earlier time, being diluted by infalling disk galaxies in increasing numbers working out from the cluster center. Any mechanism for converting spiral galaxies to S0's that is more efficient with increasing density would account qualitatively for the  $T - \Sigma$  relation observed at  $z \sim 0.5$  and  $z \sim 0$ . In this connection it is interesting to note that in present-epoch low-concentration, irregular clusters (Fig. 3) ellipticals appear to outnumber S0's in the highest density regimes, whereas the opposite situation seems to hold for the centrally concentrated clusters. Again, the manufacture of S0's by some density-dependent process seems to be a reasonable interpretation.

What prevents this picture from being a tidy one, however, is the fact that the 5 low-concentration, more irregular clusters in our distant sample show no concentration of ellipticals towards the densest regions. Instead, they possess large numbers of ellipticals spread willy-nilly over the area surveyed. Does the gradient we see in the regular clusters mean that dilution alone by infalling galaxies has already been sufficient to set up an apparent concentration of ellipticals, or must there also be a mechanism for bringing ellipticals to what will become the dense cluster regions, and, as the Whitmore & Gilmore result suggests, even more strongly to one specific cluster center? Dynamical friction is the obvious candidate for concentrating the ellipticals as different subgroups merge, but would it be sufficiently effective? By virtue of their luminosity function, which has the brightest characteristic magnitude of the morphological types (Sandage, Binggeli, & Tammann 1985), and their high M/L ratios (Faber & Gallagher 1976), ellipticals are, on average, significantly more massive than most cluster galaxies, but it remains to be seen if the effect is sufficient to generate a substantial segregation. On the other hand, the lack of a radial gradient in the luminosity function in clusters of galaxies argues against this effect being an strong one.

This discussion begs what must be the more puzzling question: why are the irregular clusters at  $z \sim 0.5$  different in terms of their  $T - \Sigma$  relations from similar clusters today? Are any of these distant irregular clusters destined to remain so until the present epoch, in which case, mechanisms like dynamical friction and dilution through infall are certainly needed to generate trends that were not present at  $z \sim 0.5$ ? Alternatively, are these distant irregular clusters the ancestors of some of today's regular clusters? If so, the same processes must have occurred to create the  $T - \Sigma$  relation, but there must be an *additional* explanation of why irregular clusters today, which are almost certainly younger dynamically than today's regular clusters, are amalgams of groups that already have, individually, well established segregations of galaxy types. A reasonable explanation for this behavior might be that morphological segregation has occurred hierarchically over time, first for the densest, most populous groups, and then working its way down to the smaller, less dense systems. In this picture, the groups that make up the irregular clusters at  $z \sim 0.5$  had not yet undergone significant morphological segregation, but by the present epoch, even these groups, from which the Hercules cluster (Abell 2151) is now being composed, would exhibit such correlations. Observations of smaller groups at intermediate redshift will be crucial for testing this notion.

Of course, testing these schematic ideas depends on understanding which mechanisms are responsible for the manufacture and distribution of S0 galaxies and, at an earlier epoch (we believe), the ellipticals. Our sample is still too small to say with certainty that these trends are universal; a larger sample is essential to verify what we have found here. Furthermore, our present data do not include sufficient area from the outer regions of intermediate-redshift clusters, a comparison with which might allow for a discrimination between the various candidates for S0 production. In forthcoming papers we hope to throw some light on this issue through the application of our large sample of spectroscopic data and what it tells us about the history of star formation in these distant cluster galaxies.

It is clearly also the case that a push to higher redshift could be very revealing: it would seem probable, based on what we have found, that the few clusters that exist at  $z \sim 1$  will show little morphological segregation of any kind. Also, by filling in the evolutionary sequence of clusters at  $z \sim 0.2$  with morphological types and colors, the progression of cluster evolution, particularly for the irregular clusters, might be better understood.

## 6. Conclusions

We have revisited the relation between morphology and surface density and confirmed that it is a fundamental characteristic of all nearby clusters and groups. However, for a sample of distant clusters,  $z \sim 0.5$ , studied with HST, the  $T - \Sigma$  relation is apparent only in high concentration, regular clusters that are presumably dynamically evolved. No correlation is found for less evolved, low concentration, irregular clusters. This suggests that the mechanisms that produce morphological segregation, either directly, by dynamical friction, for example, or through converting one type of galaxy into another, may work at different rates depending on the mass scale of the group or cluster. By the present epoch, even the smaller groups, presently coalescing to form today’s irregular clusters, may have accomplished a morphological segregation that was absent only 1/3 of a Hubble time ago.

The large number of elliptical galaxies in these clusters,  $\sim 40\%$  in both regular and irregular clusters, suggests that the creation of ellipticals predates cluster virialization. If mergers are responsible for making the ellipticals that now inhabit these rich clusters, they must have been dissipationless, in the “group phase” at  $z \sim 1$ , or much earlier,  $z > 3$ , if significant dissipation and star formation were involved. In contrast, the relative paucity of S0’s in the intermediate redshift clusters suggests that many of them have indeed been added since  $z \sim 0.5$ , by mechanisms that acted on the excessive numbers, compared to today’s clusters, of spirals and irregulars.

## Acknowledgements

Firstly, we wish to thank Ray Lucas at STScI for his enthusiastic, able help in the efficient acquisition of these HST observations. AD and AO acknowledge support from NASA through

STScI grant 3857. IRS, RSE and RMS acknowledge support from the Particle Physics and Astronomy Research Council. WJC acknowledges support from the Australian Department of Industry, Science and Technology, the Australian Research Council and Sun Microsystems. This work was supported in part by the Formation and Evolution of Galaxies network set up by the European Commission under contract ERB FMRX-CT96-086 of its TMR program.

## Appendix 1: A Further Look at the $T - \Sigma$ Relation for Nearby Clusters

The  $T - \Sigma$  relation, the basis for our analysis in this paper, has been challenged as the primary correlation between galaxy type and some associated property of the galaxy clusters. Our purpose here is review briefly the derivations of this relationship and to comment on these objections.

A first step is to reexamine the raw data that led Dressler to suspect that galaxy populations are in fact correlated with local density. In Fig. 11 we show representative clusters from the samples, with the E and S0 galaxies highlighted. Although only qualitative, one can observe even in these maps that the E and S0 galaxies are clumped together much more strongly than the cluster spirals, which are spread almost uniformly over the fields. This is true not only for reasonably regular clusters, such as Abell 151, but even for clusters without a well defined, single high density region, such as Abell1631, DC0003-50, and DC0326-53, all of which are shown in Fig. 11. Although it is difficult to use  $T - \Sigma$  relations to compare individual cases, we can verify the subjective impression of the greater clumping of E and S0 galaxies by a simpler statistic, the average nearest neighbor distances for the different types. We divided the sample into two types, E+S0 galaxies, and spirals. For the clusters just listed, the mean distance (in  $h^{-1}$  Mpc) from an E or S0 galaxy to its nearest-neighbor of the same type, compared to the mean distance of “nearest-neighbor spiral galaxies” are 0.202:0.344, 0.394:624, 0.365:0.459, and 0.338:0.551, respectively. In each case the nearest-neighbor distance between spirals is substantially larger.

This result is consistent with the idea, unsubstantiated in 1980 but subsequently strongly supported by radial velocity studies, that subclustering is a real and important phenomenon in most clusters. While the change in galaxy populations with radial distance from the centers of the clusters can be seen in Fig. 2, the existence of subgroups with populations shifted towards early Hubble types, even when removed from the centers, is also apparent.

Whitmore and collaborators claim that the T-R relation is more fundamental than the  $T - \Sigma$  relation in understanding the distribution of galaxy types within a cluster. In order to evaluate this claim, it is important to remember that the  $T - \Sigma$  and T-R relations are nearly degenerate for those clusters with a reasonably smooth, regular distribution of cluster galaxies. In such cases local surface density correlates very well with clustocentric radius. Since the remaining variations are statistical and not representative of substantial subclustering, there is no reason to expect to be able to distinguish between the two candidates for a fundamental relationship. Thus, it is essential to compare these relationships for both centrally concentrated regular clusters *and* clumpy, irregular clusters to compare the efficacy of local density or distance from the cluster center as a driver of galaxy type.

Such a comparison was the basis of Dressler’s claim that the  $T - \Sigma$  relation is universal, in the sense that it held irrespective of other global parameters. For example, Dressler noted that the  $T - \Sigma$  relations for the high-concentration and low concentration clusters were very similar, perhaps indistinguishable within sampling errors. In order to make quantitative comparisons between the relations of Fig. 2, we have fit the slopes and intercepts of the elliptical and spiral fractions as a function of  $\Sigma$ . For Figs. 2a and 2b respectively we find that the  $f(E) =$

$0.061(0.069) + 0.122(0.026)\Sigma$  and  $f(E) = 0.094(0.041) + 0.090(0.039)\Sigma$  (with  $1\sigma$  errors given in parentheses), thus confirming the impression that these cannot be distinguished within the errors. For the spirals,  $f(\text{Sp}) = 0.623(0.044) - 0.250(0.030)\Sigma$  for Fig. 2a and  $f(\text{Sp}) = 0.642(0.069) - 0.184(0.058)\Sigma$  for Fig. 2b, which indicates a marginally significant difference in the sense of a lower fraction of spirals, and a higher fraction of elliptical and S0 galaxies at a given density for the high-concentration sample. This difference might suggest a dependence on the cluster type, a global parameter, in addition to the  $T - \Sigma$  relation, but the evidence is weak.

While the  $T - \Sigma$  relation holds to first order for both regular and irregular clusters, the T-R relation explored by Whitmore and collaborators shows very different behavior in the two types of clusters. In Fig. 12 we show the T-R relation for the same samples of Fig. 2, using center positions defined by the peak in local galaxy density over the field (values taken from Beers and Tonry 1986). As found by those studies, the T-R relation for the centrally concentrated clusters is strong. In contrast, the relationship for irregular clusters of low concentration is weak. In fact, it is arguably absent except for the points within 0.5 Mpc, which result from the peaking up on a local density enhancement, in which domain one would expect the  $T - \Sigma$  relation to be again apparent, which it is. Our interpretation of Fig. 12 is, then, that application of the T-R has weakened or even eliminated a true  $T - \Sigma$  dependence further out in the cluster, by angular smoothing within the annular rings out what genuine variations do exist, leaving only the sharp gradients in the central region. Whitmore and collaborators have used the flat-to-steep profile to argue that the T-R relation is the fundamental one, but our analysis here argues, as did Dressler, that the dependence on distance from a single cluster center is only a second-order, though likely important supplement to the more fundamental correlation with local density.

That fact that the  $T - \Sigma$  relation holds for both types of clusters, and the T-R relation is substantially different for the two types, remains the best evidence that it local density is fundamental to the determination of galaxy type.

A further challenge has been made by Sanroma & Salvador-Sole (1990). These authors used angular scrambling of the galaxy positions in DCAT80 to argue that that, for the entire sample, the  $T - \Sigma$  does not exist, but is instead a derivative of the T-R relation. Again, separating centrally concentrated from low-concentration clusters is important. We have repeated this experiment for the samples of Fig. 2, scrambling around both "density peak" and "median" centers. The ranges in the distributions in density are largely maintained by the scrambling procedure, so a Kolmogorov-Smirnov test can be applied. We find that scrambling the centrally concentrated clusters produces no significant change in the  $T - \Sigma$  relation: the fraction of E galaxies at a given projected density for the real data would match that of the scrambled data 38% of the time, and the spiral fraction would match 18% of the time. In stark contrast, the  $T - \Sigma$  relation for the low-concentration clusters is in fact destroyed by the scrambling: all probabilities are  $< 10^{-4}$ , regardless of choice of galaxy center.

It is our contention, then, that the  $T - \Sigma$  relation remains important for understanding the distribution of morphological types in present-epoch clusters. This is not to say that there are no global dependences of cluster population, as Whitmore and collaborators, Sanroma & Salvador-Sole, Oemler, and even Dressler himself have suggested. In fact, in addition to the



evidence mentioned above, both Whitmore & Gilmore’s T-R relation, and the scrambling analysis of Salvadore-Sole, provide substantive evidence for global components. As can be seen in Fig. 5 of Whitmore & Gilmore (1991), the percentage of elliptical galaxies rises even higher, with a compensating *drop* in the S0 population, for those galaxies closest to the cluster center as defined by the presence of a “D” galaxy, compared to the bin of highest density of the  $T - \Sigma$  relation.<sup>¶</sup> The same can perhaps be inferred from our experiments of scrambling the clusters of the high-concentration sample and comparing the  $T - \Sigma$  relation to that of the real data. It appears that when all but the centrally located high-density peak are eliminated by the scrambling, the E fraction rises and the S0 fraction falls, as if the central location of these galaxies has an additional effect on the population. So, it appears that central location may indeed influence a galaxy’s morphology, and be perhaps an important “second-parameter” to the  $T - \Sigma$  relation.

## Appendix 2: Tabulations of $T - \Sigma$ relations

In Table 2 we tabulate the values of the  $T - \Sigma$  relations in the figures, as well as their errors. The errors stated in Table 2 are 1 sigma errors derived from Poisson statistics, assuming that the number of galaxies of a given type is independent of the number of galaxies of other types. It is also assumed that the number of background galaxies has a Poisson distribution (i.e. that the angular correlation function of galaxies is negligible at these magnitudes.)

---

<sup>¶</sup>One might have suspected that increasing the resolution of the  $T - \Sigma$  relation, by decreasing the “kernel” size to a smaller number of neighbors, would have revealed this same effect for the densest regions. However, our tests indicate that reducing to 5 neighbors does not significantly alter the fractions.

TABLE 1  
CLUSTER SAMPLE AND PROPERTIES

Cluster	RA(J2000)	DEC(J2000)	$z$	Filter	$M_{\text{lim}}$	Ngal	% E:S0:Sp	Conc.
A370#2	02:40:01.1	-01:36:45	0.37	F814W	21.98	71	28:20:52	—
Cl1446+26	14:49:28.2	+26:07:57	0.37	F702W	22.24	107	31:26:43	0.30
Cl0024+16	00:26:35.6	+17:09:43	0.39	F814W	22.11	170	37:24:39	0.53
Cl0939+47	09:43:02.6	+46:58:57	0.41	F702W	22.48	124	31:24:45	0.34
Cl0939+47#2	09:43:02.5	+46:56:07	0.41	F814W	22.23	72	35:07:58	—
Cl0303+17	03:06:15.9	+17:19:17	0.42	F702W	22.54	93	39:19:42	0.31
3C295	14:11:19.5	+52:12:21	0.46	F702W	22.76	87	51:21:28	0.58
Cl0412–65	04:12:51.7	-65:50:17	0.51	F814W	22.77	91	47:07:46	0.30
Cl1601+42	16:03:10.6	+42:45:35	0.54	F702W	23.20	100	33:12:55	0.34
Cl0016+16	00:18:33.6	+16:25:46	0.55	F814W	22.96	193	58:15:27	0.49
Cl0054–27	00:56:54.6	-27:40:31	0.56	F814W	23.00	119	34:18:48	0.38

TABLE 2  
DATA FOR FIGURE 1

$\Sigma$	f(E)	$\sigma$	f(S0)	$\sigma$	f(Sp)	$\sigma$
-0.05	0.000	0.000	0.460	0.148	0.540	0.148
0.15	0.110	0.039	0.289	0.053	0.601	0.059
0.35	0.090	0.021	0.320	0.032	0.589	0.034
0.55	0.119	0.016	0.346	0.023	0.535	0.025
0.75	0.133	0.014	0.348	0.020	0.519	0.021
0.95	0.177	0.014	0.391	0.018	0.432	0.019
1.15	0.182	0.014	0.425	0.018	0.392	0.018
1.35	0.196	0.015	0.443	0.019	0.361	0.018
1.55	0.225	0.018	0.473	0.021	0.302	0.020
1.75	0.287	0.024	0.454	0.026	0.259	0.023
1.95	0.376	0.033	0.448	0.034	0.176	0.026
2.15	0.398	0.050	0.521	0.051	0.081	0.028
2.35	0.360	0.096	0.561	0.100	0.079	0.055
2.55	0.500	0.134	0.429	0.132	0.071	0.069

DATA FOR FIGURE 2A

$\Sigma$	f(E)	$\sigma$	f(S0)	$\sigma$	f(Sp)	$\sigma$
-0.05	0.000	0.000	0.589	0.250	0.411	0.250
0.15	0.105	0.065	0.241	0.088	0.654	0.099
0.35	0.106	0.040	0.362	0.061	0.532	0.064
0.55	0.121	0.034	0.386	0.050	0.493	0.052
0.75	0.155	0.036	0.379	0.048	0.466	0.050
0.95	0.215	0.038	0.412	0.045	0.373	0.045
1.15	0.156	0.035	0.498	0.049	0.345	0.047
1.35	0.208	0.043	0.524	0.053	0.269	0.048
1.55	0.201	0.042	0.563	0.052	0.236	0.045
1.75	0.331	0.046	0.506	0.048	0.163	0.036
1.95	0.435	0.069	0.416	0.068	0.149	0.050
2.15	0.305	0.096	0.610	0.102	0.085	0.059
2.35	0.364	0.146	0.547	0.151	0.089	0.088

DATA FOR FIGURE 2B

$\Sigma$	f(E)	$\sigma$	f(S0)	$\sigma$	f(Sp)	$\sigma$
-0.05	0.149	0.242	0.595	0.328	0.256	0.316
0.15	0.177	0.112	0.234	0.135	0.589	0.153
0.35	0.113	0.066	0.192	0.079	0.695	0.093
0.55	0.153	0.049	0.318	0.062	0.529	0.067
0.75	0.169	0.038	0.298	0.047	0.533	0.051
0.95	0.181	0.036	0.364	0.046	0.454	0.048
1.15	0.180	0.031	0.457	0.040	0.363	0.039
1.35	0.189	0.034	0.459	0.043	0.351	0.042
1.55	0.252	0.055	0.393	0.062	0.355	0.061
1.75	0.318	0.108	0.369	0.112	0.313	0.108
1.95	0.481	0.101	0.280	0.090	0.238	0.086
2.15	0.501	0.251	0.499	0.251	0.000	0.000

DATA FOR FIGURE 3A

$\Sigma$	f(E)	$\sigma$	f(S0)	$\sigma$	f(Sp)	$\sigma$
0.35	0.087	0.137	0.447	0.215	0.466	0.221
0.55	0.043	0.051	0.537	0.130	0.420	0.130
0.75	0.121	0.050	0.458	0.076	0.421	0.076
0.95	0.197	0.044	0.414	0.054	0.389	0.054
1.15	0.250	0.037	0.463	0.043	0.287	0.040
1.35	0.198	0.026	0.527	0.033	0.276	0.030
1.55	0.243	0.026	0.509	0.031	0.248	0.027
1.75	0.302	0.030	0.430	0.033	0.268	0.029
1.95	0.394	0.039	0.438	0.040	0.169	0.030
2.15	0.367	0.057	0.550	0.059	0.084	0.033
2.35	0.409	0.105	0.546	0.106	0.045	0.045

DATA FOR FIGURE 3B

$\Sigma$	f(E)	$\sigma$	f(S0)	$\sigma$	f(Sp)	$\sigma$
0.55	0.000	0.000	0.524	0.298	0.476	0.298
0.75	0.096	0.100	0.375	0.170	0.529	0.177
0.95	0.099	0.103	0.517	0.171	0.384	0.169
1.15	0.308	0.132	0.542	0.143	0.149	0.105
1.35	0.174	0.051	0.577	0.068	0.249	0.060
1.55	0.202	0.044	0.546	0.055	0.252	0.049
1.75	0.331	0.048	0.492	0.051	0.177	0.039
1.95	0.432	0.070	0.433	0.070	0.135	0.049
2.15	0.263	0.101	0.685	0.107	0.052	0.052
2.35	0.364	0.146	0.547	0.151	0.089	0.088

DATA FOR FIGURE 3C

$\Sigma$	f(E)	$\sigma$	f(S0)	$\sigma$	f(Sp)	$\sigma$
0.95	0.168	0.163	0.344	0.205	0.489	0.219
1.15	0.158	0.062	0.509	0.085	0.333	0.081
1.35	0.216	0.070	0.492	0.085	0.292	0.078
1.55	0.159	0.060	0.476	0.082	0.365	0.080
1.75	0.335	0.112	0.334	0.113	0.331	0.113
1.95	0.480	0.105	0.261	0.092	0.259	0.092
2.15	0.501	0.251	0.499	0.251	0.000	0.000

DATA FOR FIGURE 4

$\Sigma$	f(E)	$\sigma$	f(S0)	$\sigma$	f(Sp)	$\sigma$
1.35	0.437	0.159	0.137	0.090	0.426	0.186
1.55	0.355	0.100	0.238	0.087	0.407	0.126
1.75	0.334	0.054	0.138	0.039	0.528	0.061
1.95	0.318	0.036	0.184	0.030	0.498	0.041
2.15	0.370	0.033	0.182	0.026	0.448	0.036
2.35	0.478	0.041	0.216	0.033	0.305	0.041
2.55	0.485	0.055	0.184	0.041	0.331	0.055
2.75	0.770	0.084	0.230	0.084	0.000	0.000

DATA FOR FIGURE 6

$\Sigma$	f(E)	$\sigma$	f(S0)	$\sigma$	f(Sp)	$\sigma$
1.35	0.586	0.458	0.105	0.156	0.309	0.514
1.55	0.426	0.233	0.184	0.152	0.390	0.281
1.75	0.320	0.074	0.145	0.054	0.534	0.085
1.95	0.350	0.051	0.198	0.043	0.452	0.058
2.15	0.306	0.046	0.202	0.040	0.491	0.052
2.35	0.450	0.068	0.190	0.053	0.359	0.069
2.55	0.292	0.081	0.235	0.075	0.473	0.092

DATA FOR FIGURE 8

$\Sigma$	f(E)	$\sigma$	f(S0)	$\sigma$	f(Sp)	$\sigma$
1.35	0.260	0.166	0.176	0.149	0.564	0.217
1.55	0.317	0.120	0.264	0.119	0.419	0.158
1.75	0.388	0.102	0.134	0.068	0.478	0.113
1.95	0.315	0.060	0.157	0.048	0.528	0.069
2.15	0.447	0.055	0.187	0.041	0.366	0.059
2.35	0.520	0.055	0.247	0.046	0.233	0.052
2.55	0.603	0.068	0.152	0.047	0.245	0.064
2.75	0.751	0.090	0.249	0.090	0.000	0.000

## REFERENCES

- Andreon, S., Davoust, E., Michard, R., Nieto, J.-L. & Poulain, P. 1996 *A&AS*, 116, 429.
- Beers, T.C. & Tonry, J.L. 1986, *ApJ*, 300, 557.
- Bertin E., & Arnoults, S. 1996, *A&AS*, 117, 393.
- Bhavsar, S.P., 1981, *ApJL*, 246, L5.
- Bower, R.G., Lucey, J.R. & Ellis, R.S., 1991, *MNRAS*, 254, 601.
- Butcher, H., & Oemler, A. Jr. 1978, *ApJ*, 226, 559.
- de Sousa, R.E., Capelato, H.V., Arakaki, L, & Loguillo, C., 1982, *ApJ*, 263, 557.
- Dressler, A. 1980a, *ApJ*, 236, 351. (D80)
- Dressler, A. 1980b, *ApJS*, 424, 565. (DCAT80)
- Ellis, R.S., Smail, I., Dressler, A., Couch. W.J., Oemler, A. Jr., Butcher, H., & Sharples, R.M. 1996, *ApJ*, in press.
- Evrard, A., Silk, J., & Szalay, A.S. 1990, *ApJ*, 365, 13.
- Faber, S.M, & Gallagher, J.S., 1976, *ApJ*, 204, 668.
- Geller, M.J, and Beers, T.C. 1982, *PASP*, 94, 421.
- Giovanelli, R., Haynes, M.P., & Chincarini, G.L. 1986, *ApJ*, 300, 77.
- Griffiths, R.E., Casertano, S., Ratnatunga, K.U., Neuschaefer, L.W., Ellis, R.S., Gilmore, G.F., Glazebrook, K. Santiago, B., Huchra, J.P., et al. 1994, *ApJ*, 435, L19.
- Gunn, J.E., & Gott, J.R. 1972, *ApJ*, 176, 1.
- Holtzman, J.A., Burrows, C.J., Casertano, S., Hester, J.J., Trauger, J.T., Watson, A.M. & Worthey, G. 1995, *PASP*, 107, 1065.
- Hubble, E., & Humason, M.L. 1931, *ApJ*, 74, 43.
- Melnick, J., & Sargent, W.L.W., 1977, *ApJ*, 215, 401.
- Moore, B., Katz, N., Lake, G., Dressler, A., and Oemler, A. Jr. 1996, *Nature*, 379, 613.
- Oemler, A. Jr., 1974, *ApJ* 194, 1.
- Oemler, A. Jr., Dressler, A., and Butcher, H. 1997, *ApJ*, 474, 561.
- Postman, M., & Geller, M.J., 1984, *ApJ*, 281, 95.
- Salvador-Sole, E. Sanroma, M., and Rdz.Jordana, J.J. 1989, *ApJ*, 337, 636.
- Sandage, A., Binggeli, B., and Tammann, G.A. 1985, *AJ*, 90, 395.
- Sandage, A., Freeman, K.C., & Stokes, N.R. 1970, *ApJ*, 160, 831.
- Sanroma, M., & Salvador-Sole, E., 1990, *ApJ*, 360, 16.
- Smail, I., Dressler, A., Couch, W.J., Ellis, R.S., Oemler, A. Jr., Butcher, H. & Sharples, R.M. 1996a, *ApJ*, in press. (S97a)

Smail, I., Ellis, R.S., Dressler, A., Couch, W.J., Oemler, A. Jr., Sharples, R.M, & Butcher, H. 1996b, ApJ 479, 70.

Spitzer, L., and Baade, W. 1951, ApJ, 113, 413.

Whitmore, B.C., & Gilmore, D.M., 1991, ApJ, 367, 64.

Whitmore, B.C., Gilmore, D.M., & Jones, C. 1993, ApJ, 407, 489.

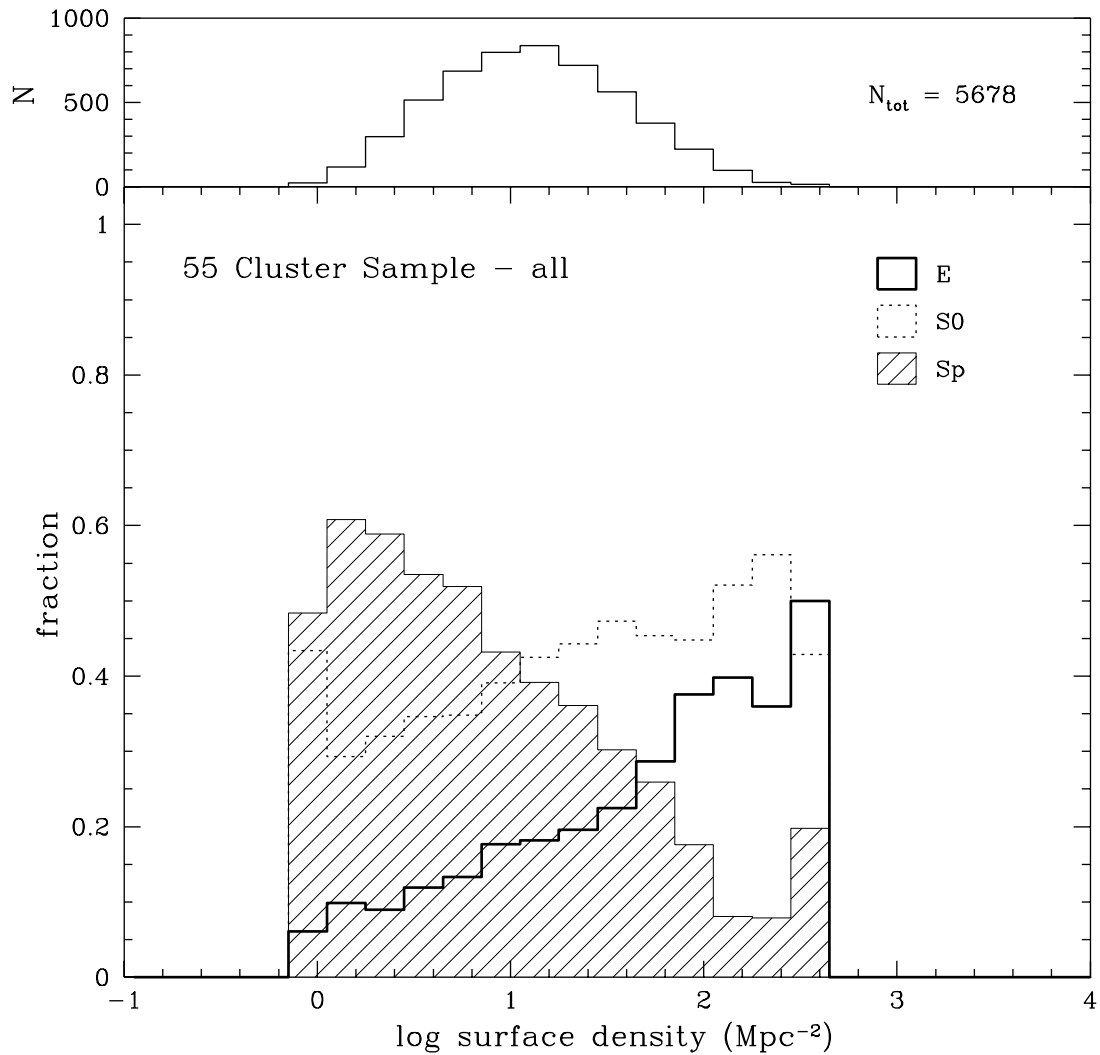


**Figure 1.** The  $T - \Sigma$  (morphology-density) relation for the D80 55 cluster sample, reanalyzed, as discussed in the text. The histogram at the top shows the numbers of galaxies in each bin of surface density, for the total number in the upper right corner.



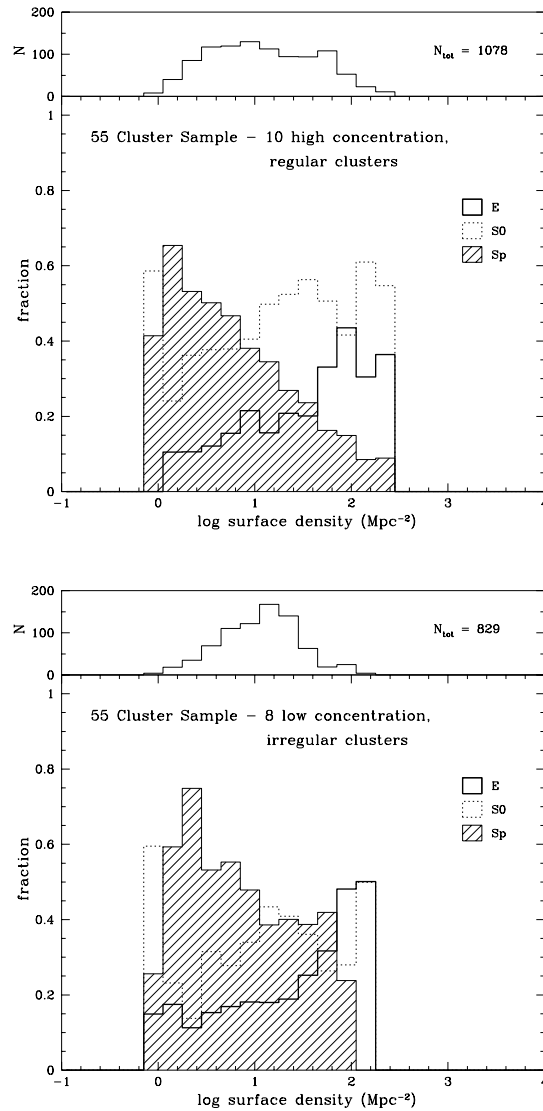


**Figure 2.** The  $T - \Sigma$  relation for 10 centrally concentrated, regular clusters of the D80 cluster sample (above), A151, A539, A957, A1656, A1913, A2040, A2063, DC0247-31, DC0428-53, DC1842-63, and (below), 8 low-concentration clusters A76, A119, A168, A978, A979, A1644, A2151, and DC0003-50.

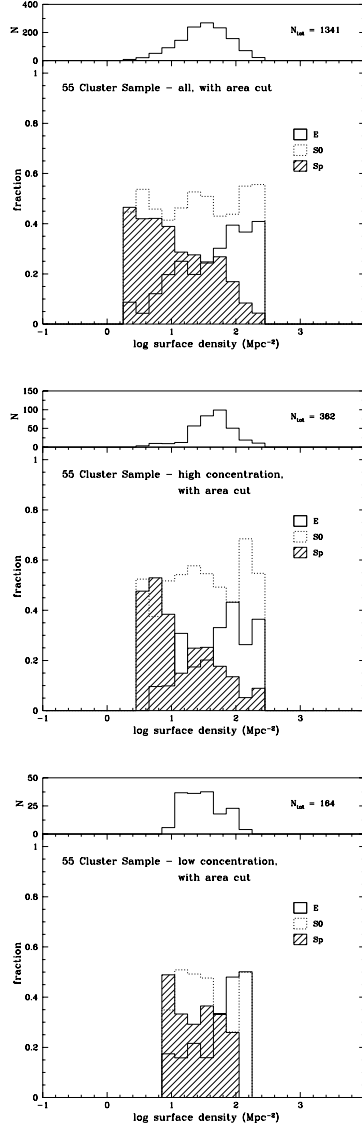


**Figure 3.** The  $T - \Sigma$  relation for all 55 clusters of the D80 cluster sample, but limited to a smaller area of 1.2 Mpc, comparable to that covered by the more distant HST sample. From top to bottom: all clusters; centrally-concentrated clusters, low-concentration clusters.

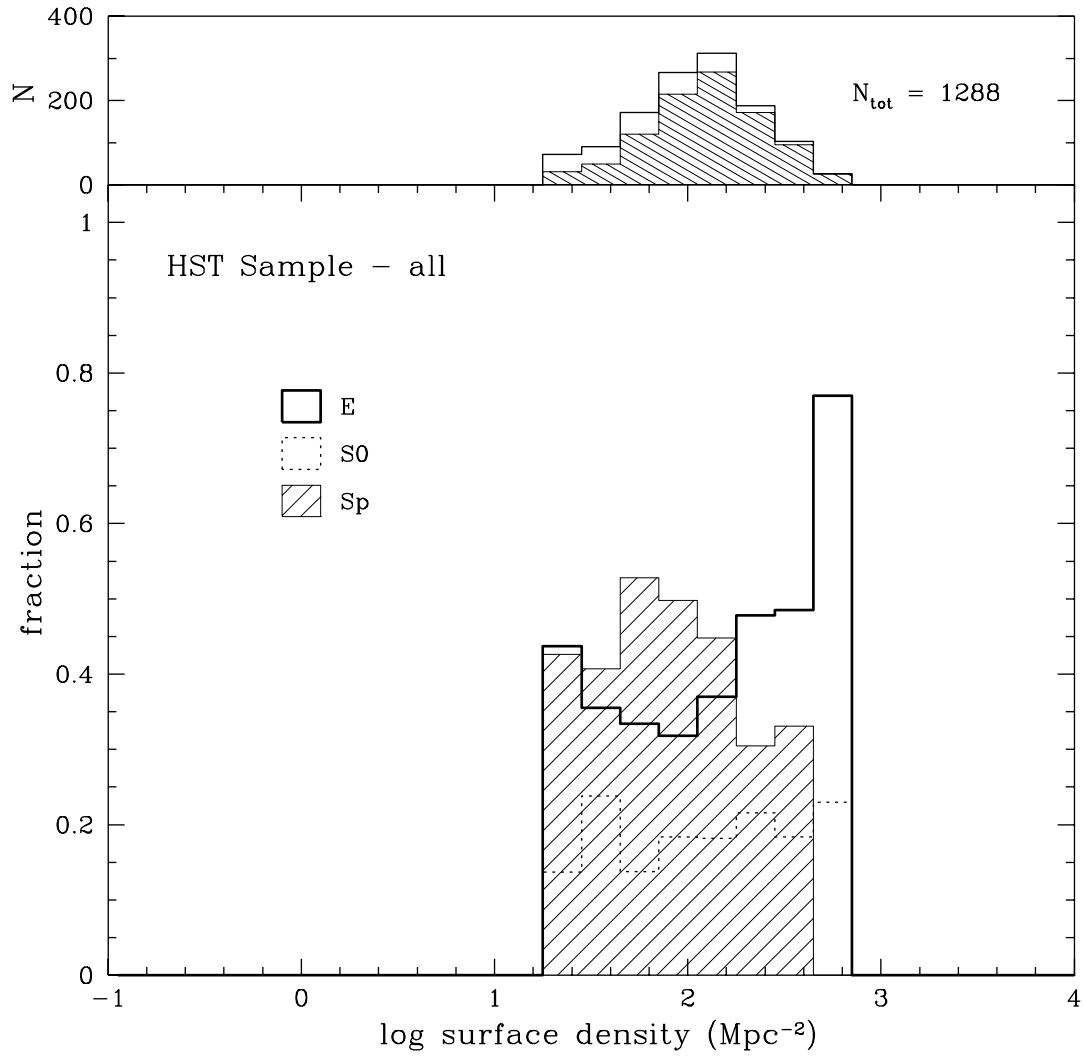


**Figure 4.** The  $T - \Sigma$  relation for 10 clusters at intermediate redshift,  $0.36 < z < 0.57$ . The histogram in the top box shows the number of galaxies in each bin, with the shaded portion indicating the number after correcting for field contamination.

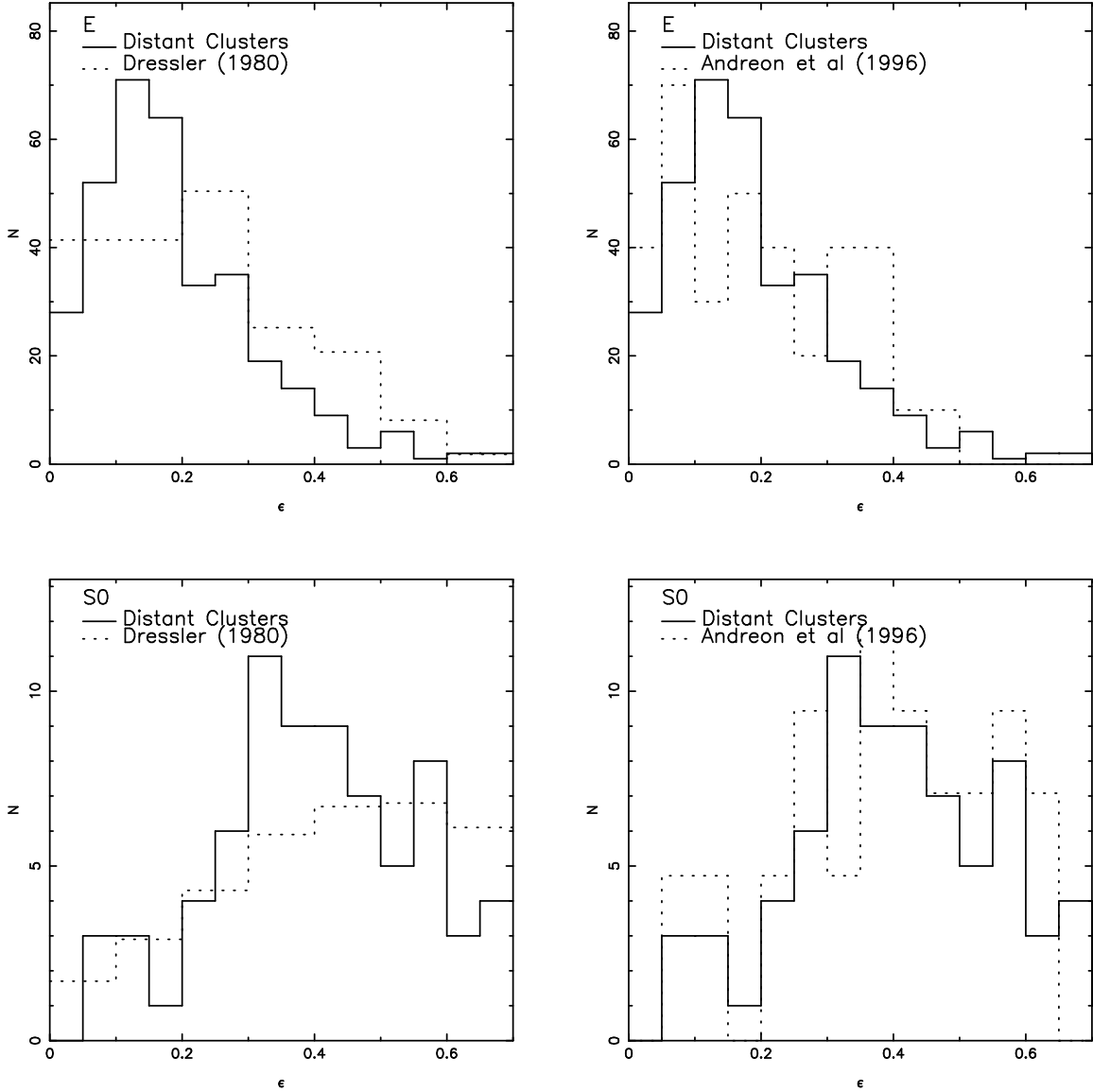


**Figure 5.** The distribution of ellipticities for E and S0 galaxies in the  $z \sim 0.5$  sample compared to that for the Coma cluster (Andreon et al. 1996) and for 11 clusters  $0.035 < z < 0.044$  of the Dressler (1980) low redshift sample. The similarity of these distributions suggests that a fair comparison of the fraction of E and S0 galaxies can be made between  $z \sim 0$  and  $z \sim 0.5$ .

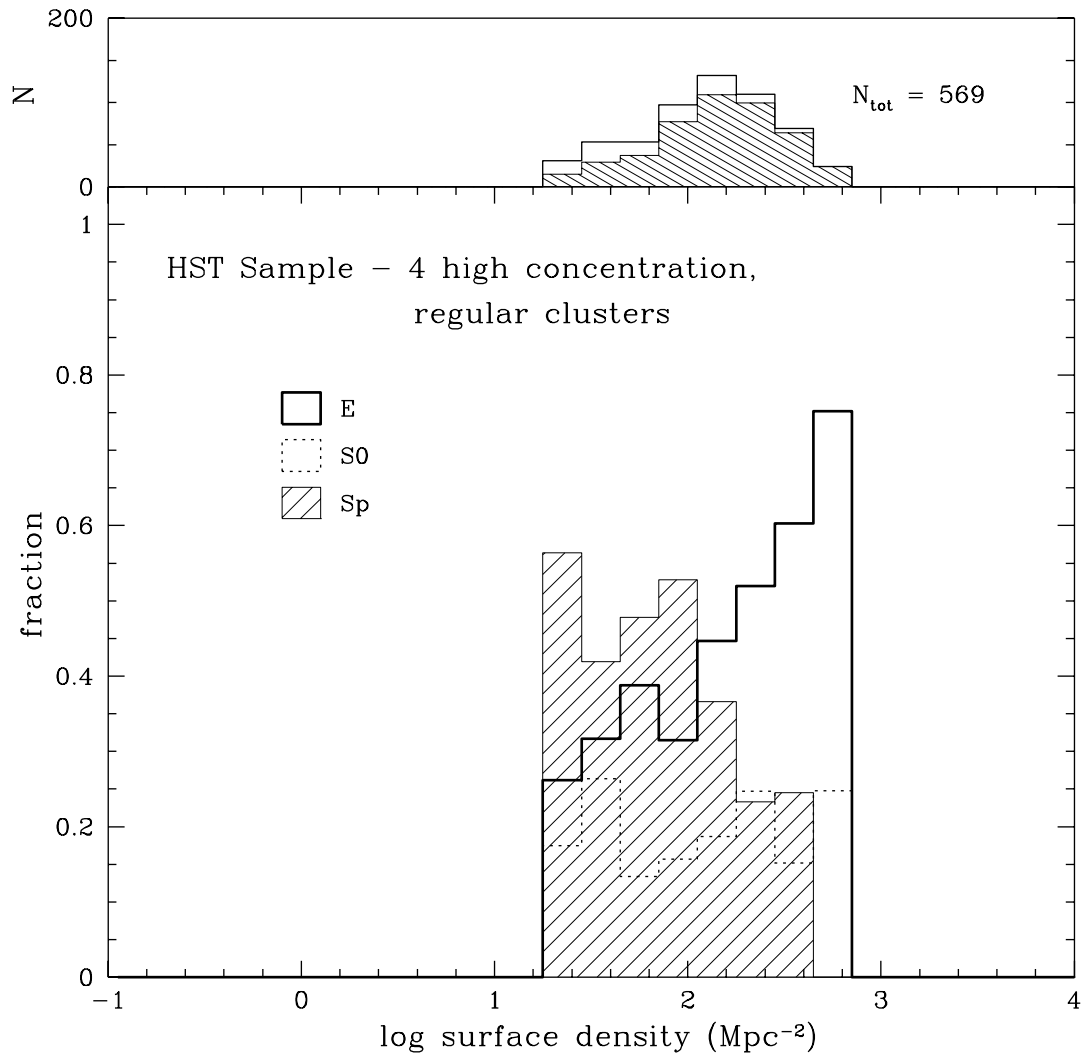


**Figure 6.** The  $T - \Sigma$  relation for 4 centrally concentrated, regular clusters at intermediate redshift, 3C295, Cl0016+16, Cl0024+16, and Cl0054-27.

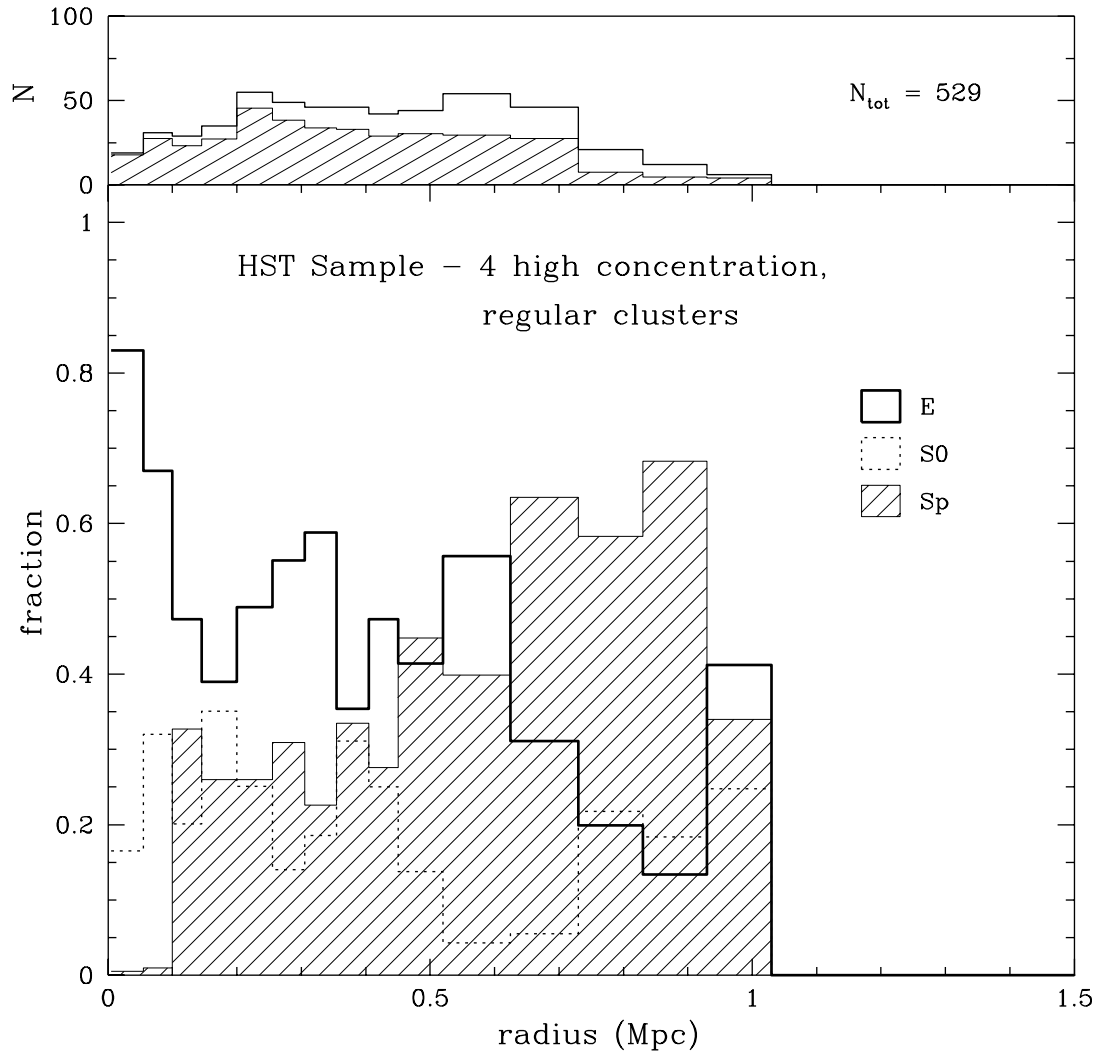


**Figure 7.** The T-R (morphology-clustocentric radius) relation for 4 high-concentration, regular clusters at intermediate redshift, 3C295, Cl0016+16, Cl0024+16, and Cl0054-27.

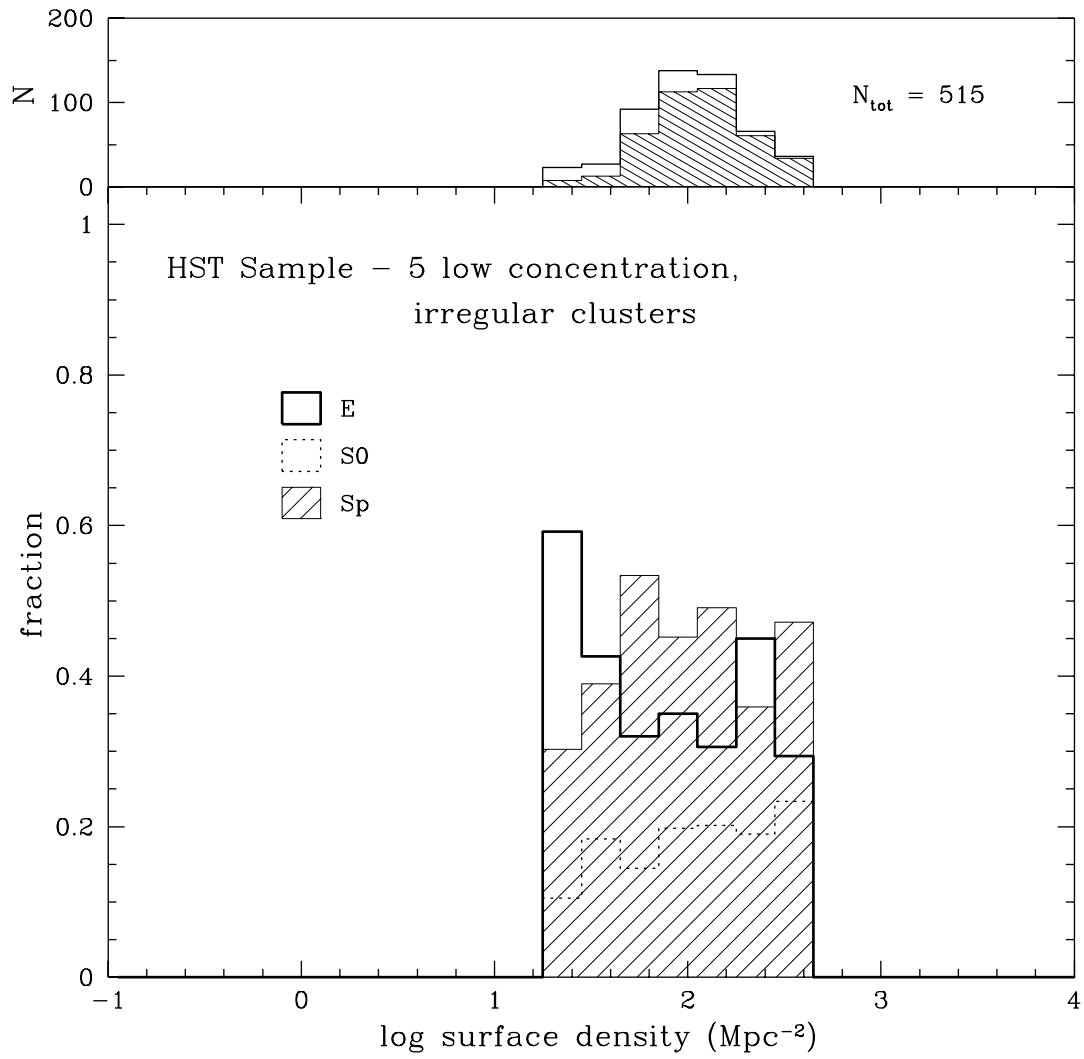


**Figure 8.** The  $T - \Sigma$  relation for 5 low-concentration, irregular clusters at intermediate redshift, Cl0303+17, Cl0412-65, Cl0939+47, Cl1447+23, and Cl1601+42.

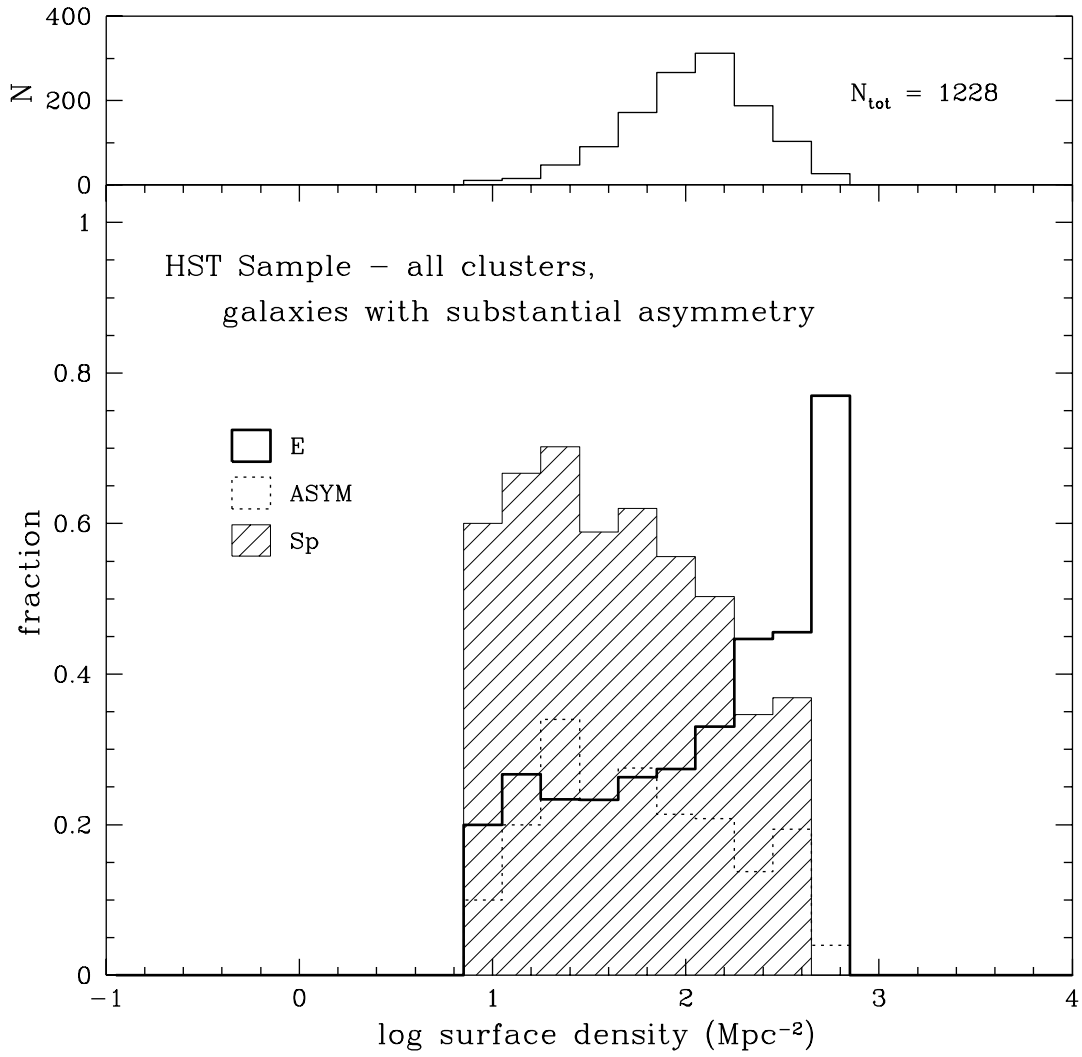


**Figure 9.** The  $T - \Sigma$  relation for 10 clusters at intermediate redshift, including those galaxies with substantial asymmetry or disturbance, irrespective of morphological type. These galaxies follow the spiral or S0 trend rather than the elliptical trend.



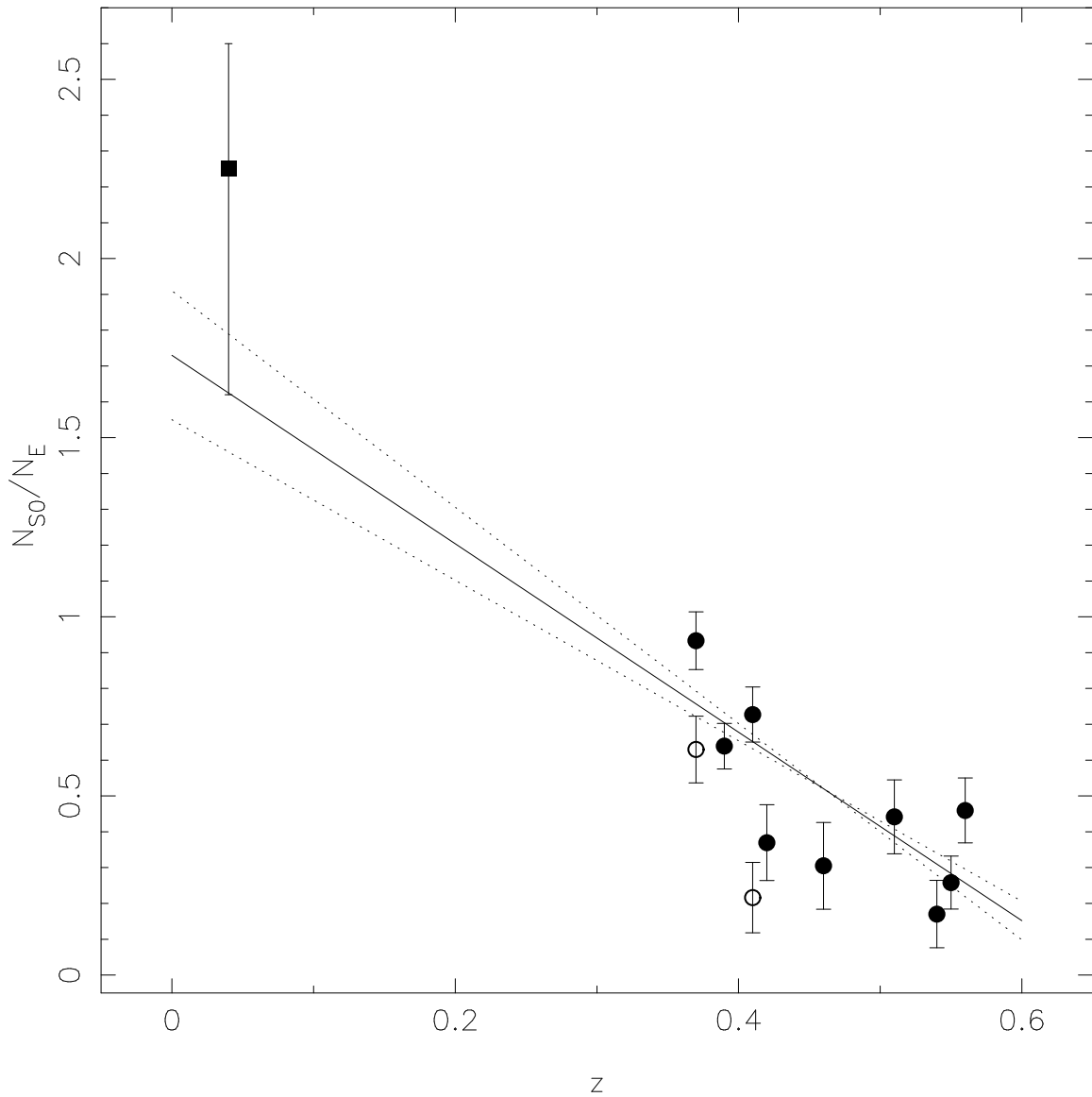


**Figure 10.** The S0/E fraction for clusters in the sample as a function of redshift. The open circles are the outer fields in A370 and Cl0939+47, which are not used in the least-squares fit, shown with its  $1\text{-}\sigma$  errors as the solid and dotted lines. The extrapolation of this linear relation to zero redshift approximately matches the value  $S0/E \sim 2$ , shown by the solid box, found for 11 clusters  $0.035 < z < 0.044$  of the D80 cluster sample.

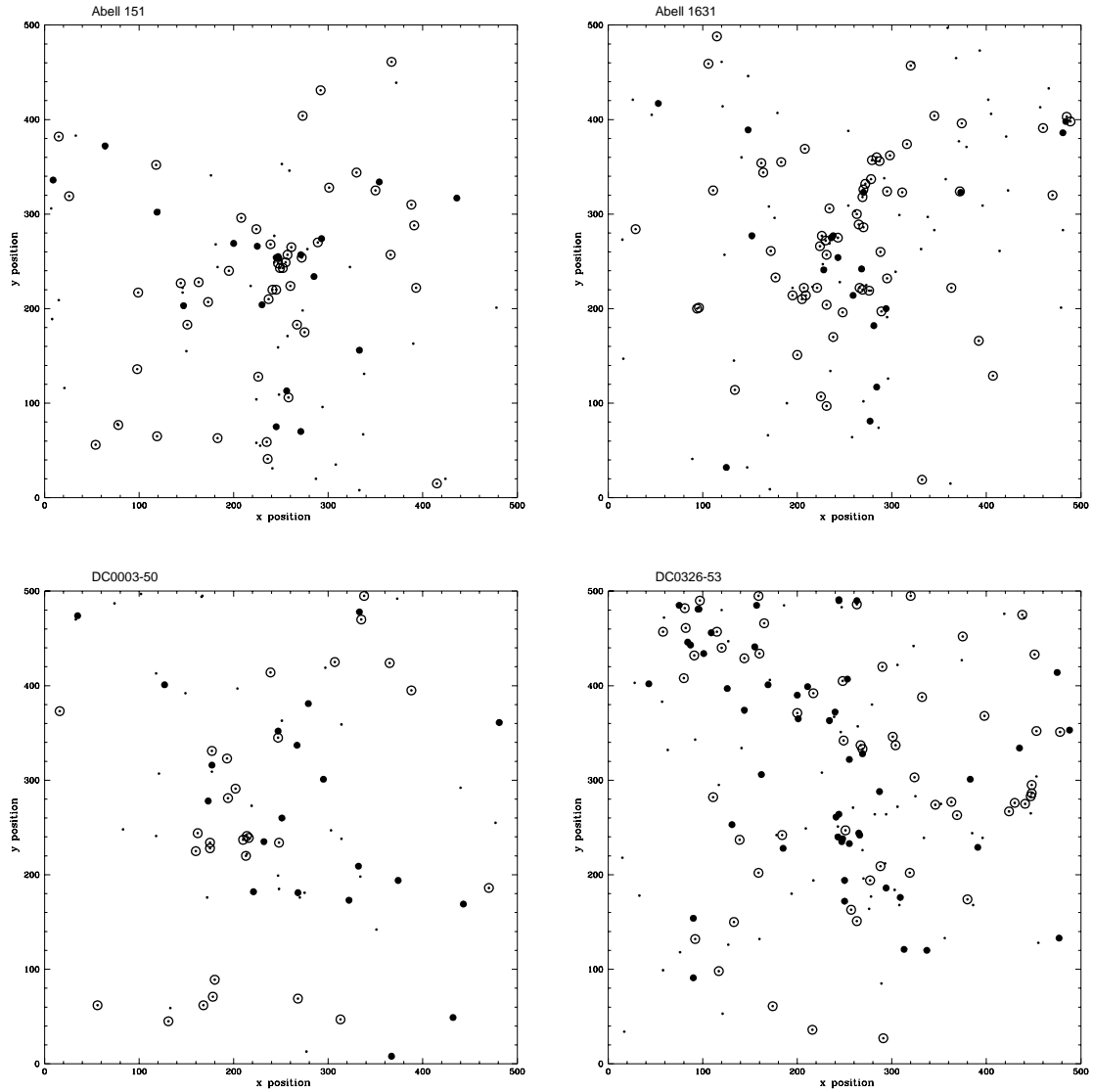


**Figure 11.** Maps showing the positions of galaxies in four clusters of the D80 55 cluster sample, A151, A1631, DC0003-50, and DC0326-53. Large solid dots are elliptical galaxies, dotted-circles are S0's, and small dots are spirals. The enhanced clustering of E and S0 galaxies compared to spirals is evident.

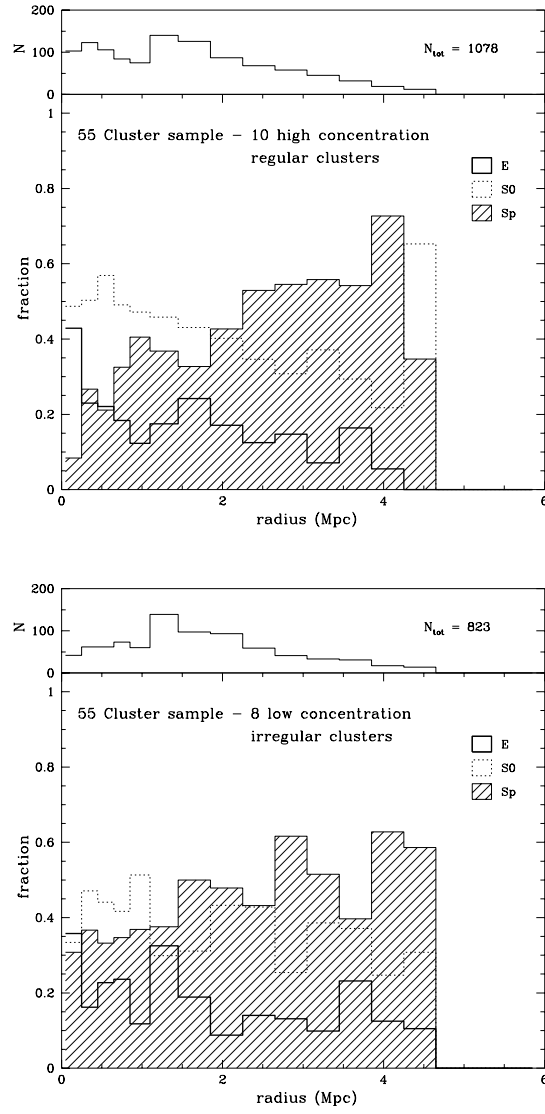


**Figure 12.** The T-R relation for the same clusters of Fig. 3. As expected, population gradients are strong for centrally concentrated clusters (above), and weak or absent for low-concentration irregular clusters.